

β -function for topologically massive gluons

Debmalya Mukhopadhyay* and Amitabha Lahiri†

*S.N. Bose National Centre of Basic Science, Sector-III, Block-JD,
Saltlake, Kolkata, West Bengal
India.*

October 29, 2018

Abstract

We calculate the quantum corrections to the two-point function of four dimensional topologically massive non-Abelian vector fields at one loop order for $SU(N)$ gauge theory in Feynman-'t Hooft gauge. We calculate the beta function of the gauge coupling constant and find that the theory becomes asymptotically free faster than pure $SU(N)$ gauge theory.

1 Introduction

The recent discovery of a 125-GeV Higgs boson [1, 2] has completed the observation of the fundamental particles of the Standard Model [3, 4]. But it has not completed the description of the low energy particle universe. The mechanism for neutrino masses remains incompletely understood, as does the mechanism of family symmetry breaking. There may be more particles lurking in the shadows not yet illuminated by the LHC, if not superpartners, then at least the particles that make up dark matter.

The mechanism of color confinement also remains unknown. It is not clear if the LHC will be able to shed any light on this problem, since confinement

*debmalya@bose.res.in

†amitabha@bose.res.in

occurs at low energy, and quarks and gluons are effectively free particles at the energies probed by the LHC. However, the LHC may be able to answer a related question, that of whether strong interactions, which are short-range like the weak interactions, are also mediated by massive vector bosons. The idea of a dynamically generated gluon mass has been at the root of much recent activity (see e.g. [5] and references therein). It has been known for a long time that such a mass provides a qualitative understanding of many dimensionful parameters of QCD, including the string tension [6]. In fact a gauge-invariant mass of the gluon is just as useful [7], and plays an important role in the center-vortex picture of confinement [8]. In this picture, vortices of thickness $\sim m^{-1}$, and carrying magnetic flux in the center of the gauge group, are assumed to form a condensate, where m is the mass of the gauge boson. For fundamental Wilson loops that are large compared to m^{-1} an area law can be shown to arise, although loops of size $\sim m^{-1}$ obey a perimeter law. However, unbroken Yang-Mills theory with massive gluons is generally believed to be not renormalizable.

In this paper we consider a special kind of gauge-invariant mass, namely topologically generated gluon mass, which generalizes the similarly named Abelian mechanism [9]. In this model, the field strength F of the gauge field is coupled to an antisymmetric tensor potential B via a term of the form $\epsilon^{\mu\nu\rho\lambda}\text{Tr} B_{\mu\nu}F_{\rho\lambda}$. A kinetic term for the B field is also included, leading to the gauge field propagator developing a pole. The model does not require spontaneous symmetry breaking, can be shown to be unitary [10, 11, 12], and there is good reason to believe that it is also renormalizable in an algebraic sense [13], but it is not known if this massive theory remains asymptotically free. In this paper we investigate how the gauge field propagator is modified at one loop by the coupling with the tensor field, and calculate the beta function of gauge coupling constant.

In pure Yang-Mills theory with gauge group $SU(N)$, the coupling constant at one loop runs with energy as

$$\alpha(Q^2) = \frac{\alpha(\mu^2)}{1 + N \frac{11}{12\pi} \alpha(\mu^2) \ln \frac{Q^2}{\mu^2}}, \quad (1)$$

where μ is the renormalization point, and α is related to the gauge coupling constant g by $\alpha = \frac{g^2}{4\pi}$. The corresponding beta function is then

$$\beta(\alpha) = -\frac{11}{3} N \frac{\alpha^2}{2\pi}. \quad (2)$$

When interactions with fermions or scalars are included, the beta function gets modified to

$$\beta(\alpha) = \left(-\frac{11}{3}N + nN_f \right) \frac{\alpha^2}{2\pi}, \quad (3)$$

where n is $\frac{2}{3}$ for a fermion, $\frac{1}{3}$ for a complex scalar and $\frac{1}{6}$ for a real scalar field, and N_f is the number of flavors. The positive sign before the second term in the expression in Eq. (3) signifies the screening effect due to virtual pairs of matter particles. Thus perturbation theory breaks down for sufficiently large number of species of particles, and this equation allows us to calculate the energy where it does so.

We will see below that the antisymmetric tensor has an anti-screening effect on the gauge coupling constant. This is an effect of the specific coupling considered, and we should think of the anti-screening as an effect of the gauge-invariant topological mass of the gluon. We find the result surprising, since massive gluons are short-range.

2 Feynman rules for the model

We start from the Lagrangian

$$\begin{aligned} \mathcal{L} = & -\frac{1}{4}F_a^{\mu\nu}F_{\mu\nu}^a + \frac{1}{12}H_a^{\mu\nu\lambda}H_{\mu\nu\lambda}^a + \frac{m}{4}\epsilon^{\mu\nu\rho\lambda}F_{\mu\nu}^aB_{\rho\lambda}^a \\ & + \partial_\mu\bar{\omega}_a\partial^\mu\omega^a - gf_{bca}A_\mu^b\partial^\mu\bar{\omega}^a\omega_c - \frac{1}{2\xi}(\partial_\mu A_a^\mu)^2. \end{aligned} \quad (4)$$

Here $F_a^{\mu\nu}$ is the field strength of the gauge bosons,

$$F_a^{\mu\nu} = \partial^\mu A_a^\nu - \partial^\nu A_a^\mu - gf_{bca}A_b^\mu A_c^\nu, \quad (5)$$

and $H_{\mu\nu\lambda}^a$ is the field strength of the second rank anti-symmetric field $B_a^{\mu\nu}$, given by

$$H_a^{\mu\nu\lambda} = \partial^{[\mu}B_a^{\rho\lambda]} - gf_{bca}A_b^{[\mu}B_c^{\rho\lambda]}, \quad (6)$$

where the square brackets imply sum over cyclic permutations, $\partial^{[\mu}B_a^{\rho\lambda]} = \partial^\mu B_a^{\rho\lambda} + \partial^\rho B_a^{\lambda\mu} + \partial^\lambda B_a^{\mu\rho}$. The Lagrangian density has been written in terms of the renormalized fields and coupling constants.

The quadratic in the kinetic term of $B_{\mu\nu}^a$ cannot be inverted for obtaining the propagator. We add a term invariant under $SU(N)$ gauge invariance,

$$\mathcal{L}' = \frac{1}{2\eta}(D_\mu B_a^{\mu\nu})^2, \quad (7)$$

to the Lagrangian density in Eq. (4) to get the propagator of the tensor field. Here η is a arbitrary parameter and D_μ is the gauge covariant derivative. The propagators of the fields are from the quadratic parts from the renormalised Lagrangian density and \mathcal{L}' excluding the $B \wedge F$ term, are

$$i\Delta_{\mu\nu,ab} = -\frac{i}{k^2} \left(g^{\mu\nu} - (1 - \xi) \frac{k^\mu k^\nu}{k^2} \right) \delta_{ab} \quad (8)$$

$$i\Delta_{\mu\nu,\rho\lambda;ab} = \frac{i}{k^2} \left(g_{\mu[\rho} g_{\lambda]\nu} + (1 - \eta) \frac{k_{[\mu} k_{[\lambda} g_{\rho]\nu]}}{k^2} \right) \delta_{ab} \quad (9)$$

We get a two-point coupling of gauge field and B field from the third term in the Lagrangian of Eq. (4). It causes mixing of the A field with the B field. The third term also contains an ABB interaction. The vertex rules for the two-point coupling and the three-point coupling are respectively

$$iV_{\mu\nu,\lambda}^{ab} = -m\epsilon_{\mu\nu\lambda\rho} k^\rho \delta^{ab}, \quad (10)$$

$$iV_{\mu,\nu,\lambda\rho}^{abc} = igmf^{bca} \epsilon_{\mu\nu\lambda\rho}. \quad (11)$$

The corresponding vertex diagrams are displayed in Fig. 1.

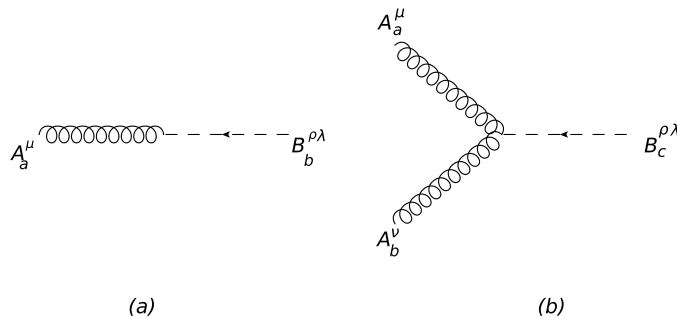


Figure 1: (a) Two-point vertex due to the AB interaction; (b) three-point vertex due to the ABB interaction.

Because of the two-point coupling, the quadratic terms in the A and B fields are not diagonal, the two-point vertex corresponds to an off-diagonal

mixing term. When calculating the propagator of the A field, one has to sum over all tree diagrams in which the B propagator is inserted into the A propagator via this two-point interaction, as shown in Fig. 2. This ‘diagonalizes’ the matrix of the propagators.

Figure 2: Sum over insertions of the B -propagator into A -propagator.

The complete propagator is given by summing the diagrams in this infinite series [9]

$$\begin{aligned} iD_{\mu\nu}^{ab} &= (i\Delta_{\mu\nu} + i\Delta_{\mu\mu'}iV_{\sigma\rho,\mu'}i\Delta_{\sigma\rho,\sigma'\rho'}iV_{\sigma'\rho',\nu'}i\Delta_{\nu'\nu} + \dots) \delta^{ab} \\ &= -i \left[\frac{g_{\mu\nu} - \frac{k_\mu k_\nu}{k^2}}{(k^2 - m^2)} + \xi \frac{k_\mu k_\nu}{k^4} \right] \delta^{ab}. \end{aligned} \quad (12)$$

Similarly, the full tree-level propagator of the $B_{\mu\nu}$ field can be obtained summing over insertions of the A -propagator via the two-point coupling,

$$iD_{\mu\nu,\rho\lambda}^{ab} = i \left[\frac{g_{\mu[\rho}g_{\lambda]\nu} + \frac{k_{[\mu}k_{[\lambda}g_{\rho]\nu]}}{k^2}}{k^2 - m^2} - \eta \frac{k_{[\mu}k_{[\lambda}g_{\rho]\nu]}}{k^4} \right] \delta^{ab}. \quad (13)$$

We will choose the Feynman-'t Hooft gauge $\xi = 1$, and put $\eta = 1$, to further simplify the calculations.

Next we consider the interactions coming from the terms quadratic in the B -field, namely the second term of Eq. (4) and the added term of Eq. (7). These terms contain ABB and $AABB$ interactions, with diagrams shown in Fig. 3. Their vertex rules are respectively

$$iV_{\mu,\lambda\rho,\sigma\tau}^{abc} = gf^{abc} \left[(p - q)_\mu g_{\lambda[\sigma}g_{\tau]\rho} + (p + q/\eta)_{[\sigma} g_{\tau][\lambda}g_{\rho]\mu} - (q + p/\eta)_{[\lambda} g_{\rho][\sigma}g_{\tau]\mu} \right], \quad (14)$$

and

$$\begin{aligned} iV_{\mu,\nu,\lambda\rho,\sigma\tau}^{abcd} &= ig^2 \left[f_{ace}f_{bde} \left(g_{\mu\nu}g_{\lambda[\sigma}g_{\tau]\rho} + g_{\mu[\sigma}g_{\tau]g[\lambda}g_{\rho]\nu} - \frac{1}{\eta}g_{\mu[\lambda}g_{\rho][\sigma}g_{\tau]\nu} \right) \right. \\ &\quad \left. + f_{ade}f_{bce} \left(g_{\mu\nu}g_{\lambda[\sigma}g_{\tau]\rho} + g_{\mu[\lambda}g_{\rho]g[\sigma}g_{\tau]\nu} - \frac{1}{\eta}g_{\mu[\sigma}g_{\tau]g[\lambda}g_{\rho]\nu} \right) \right]. \end{aligned} \quad (15)$$

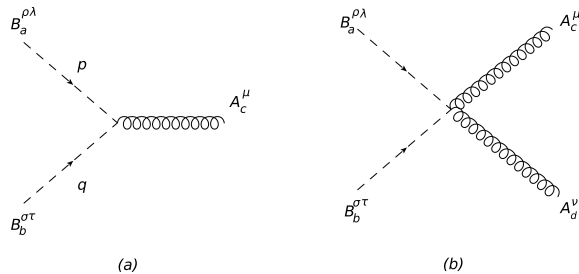


Figure 3: ABB and AABB vertices;

The gauge coupling constant g is a gauge invariant quantity, hence its variation with the energy, i.e. beta function, does not depend on the choice of gauge fixing term, in particular the value of the gauge-fixing parameter ξ . The parameter η is also unaffected by gauge transformations, so any value can be chosen for η without affecting the β -function. Therefore, as mentioned above, we choose the Feynman-'t Hooft gauge $\xi = 1$, and also put $\eta = 1$ for the simplification of the calculations.

We use dimensional regularization for the loop integrations. The integrations are done in $4 - \epsilon$ dimensions. Since our goal is to get the beta function at one-loop order, it is sufficient to calculate the coefficient of $\frac{2}{\epsilon}$ in the result of the loop-integration.

3 One loop diagrams

In this section we calculate the diagrams which contribute to the one-loop β -function for the gauge coupling constant g . We start with the diagrams which appear in pure Yang-Mills theory. These are generated only by the three and four-point couplings of the gauge and ghost fields, with the diagrams shown in Fig. 4. We should check if there are any differences in the divergent part with the known result in the literature, since we are now considering massive gauge fields rather than massless ones. It is easy to see that the divergent parts of the diagrams in Fig. 4(a) and Fig. 4(b) are different from the ordinary (massless) case, whereas the ghost loop in Fig. 4(c) remains unaffected. Denoting the four-momentum of the external legs as p^μ , we

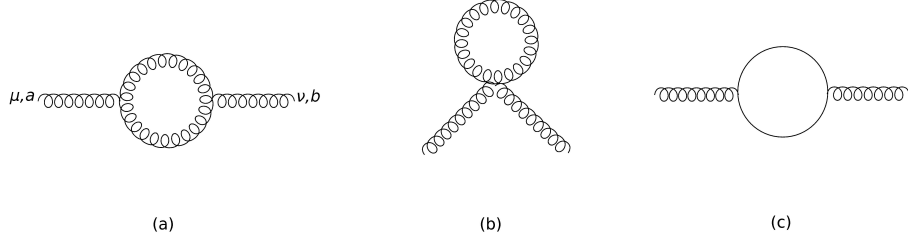


Figure 4: (a) and (b): Gluon loop; (c): ghost loop;

calculate that the divergent part for Fig. 4(a) is given by

$$\Pi_{ab,\mu\nu,\epsilon}^{4a} = \frac{1}{2} \frac{N\delta^{ab}g^2}{16\pi^2} \left[\frac{19g_{\mu\nu}p^2 - 22p_\mu p_\nu}{6} - \frac{3}{2}m^2 g_{\mu\nu} \right], \quad (16)$$

where the factor of $\frac{1}{2}$ appears due to the presence of identical gauge boson propagators in the loop. The subscript ϵ is placed on $\Pi_{ab,\mu\nu,\epsilon}^n$ to indicate that the right hand side of this equation is the coefficient of $\frac{2}{\epsilon}$. It should be obvious that the second term containing m^2 appears due to the massive pole in the internal propagator. In fact this is the only difference with the same diagram for massless gauge bosons. The divergent part for the diagram in Fig. 4(b) is calculated to be

$$\Pi_{ab,\mu\nu,\epsilon}^{4b} = -\frac{1}{4} \frac{N\delta^{ab}g^2}{16\pi^2} 9m^2 g_{\mu\nu}. \quad (17)$$

This diagram is known to vanish for massless gauge fields, as is borne out by the mass dependence of the amplitude calculated here. The contribution from the divergent part for the diagram in Fig. 4(c), which contains a ghost loop, does not change from the usual $SU(N)$ gauge theory because the Fadeev-Popov ghosts are massless. So we can write

$$\Pi_{ab,\mu\nu,\epsilon}^{4c} = -\frac{N\delta^{ab}g^2}{16\pi^2} \frac{(-g_{\mu\nu}p^2 - 2p_\mu p_\nu)}{12}. \quad (18)$$

Adding up the three contributions, we calculate the total contribution of the loops in Fig. 4,

$$\begin{aligned} \Pi_{ab,\mu\nu,\epsilon}^4 &= \Pi_{ab,\mu\nu,\epsilon}^{4a} + \Pi_{ab,\mu\nu,\epsilon}^{4b} + \Pi_{ab,\mu\nu,\epsilon}^{4c} \\ &= \frac{N\delta^{ab}g^2}{16\pi^2} \left[\frac{5}{3} (p^2 g_{\mu\nu} - p_\mu p_\nu) - 3m^2 g_{\mu\nu} \right]. \end{aligned} \quad (19)$$

We will now consider the loops based on cubic and quartic interactions between $B_{\mu\nu}$ and the gauge field A_μ , for which the vertices have been shown in Fig. 3. The three point interactions ABB and AAB lead to the loop

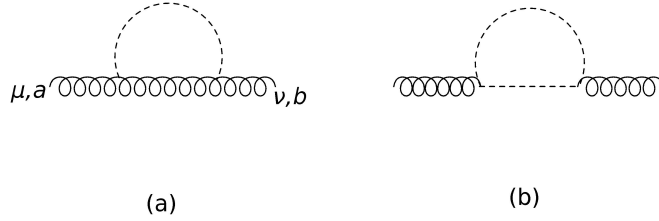


Figure 5: Loops formed by AAB and ABB couplings

diagrams shown in Fig. 5. The coefficients of $\frac{2}{\epsilon}$ from the loop integration corresponding to them are respectively

$$\Pi_{ab,\mu\nu,\epsilon}^{5a} = \frac{N\delta^{ab}g^2}{16\pi^2} 3m^2 g_{\mu\nu}, \quad (20)$$

$$\Pi_{ab,\mu\nu,\epsilon}^{5b} = \frac{N\delta^{ab}g^2}{16\pi^2} [p^2 g_{\mu\nu} - p_\mu p_\nu + 3m^2 g_{\mu\nu}]. \quad (21)$$

The propagator of the $B_{\mu\nu}$ field in the loop is the one given in Eq. (13). Adding the two contributions, we get for the loops in Fig. 5

$$\Pi_{ab,\mu\nu,\epsilon}^5 = \Pi_{ab,\mu\nu,\epsilon}^{5a} + \Pi_{ab,\mu\nu,\epsilon}^{5b} = \frac{N\delta^{ab}g^2}{16\pi^2} [p^2 g_{\mu\nu} - p_\mu p_\nu + 6m^2 g_{\mu\nu}]. \quad (22)$$

Next we consider the 1-loop diagrams generated by the cubic AAA interaction at one vertex and the AAB interaction at the other vertex. These are shown in Fig. 6, the contributions from the two diagrams are equal. The divergent part of the amplitudes corresponding to these diagrams is

$$\Pi_{ab,\mu\nu,\epsilon}^{6a} = -\frac{1}{2} \frac{N\delta^{ab}g^2}{16\pi^2} \frac{9}{4} m^2 g_{\mu\nu} = \Pi_{ab,\mu\nu,\epsilon}^{6b} \quad (23)$$

The symmetry factor $\frac{1}{2}$ appears in Fig. 6(a) and Fig. 6(b) since these diagrams contain identical internal propagators of the gauge field. In these diagrams, and in later ones, we take Eq. (13) as the propagator of $B_{\mu\nu}$ whenever an internal line of the loop contains the two point AB vertex. As before, we set $\eta = 1$. Hence the total contribution is

$$\Pi_{ab,\mu\nu,\epsilon}^6 = 2\Pi_{ab,\mu\nu,\epsilon}^{6a} = -\frac{N\delta^{ab}g^2}{16\pi^2} \frac{9}{4} m^2 g_{\mu\nu} \quad (24)$$

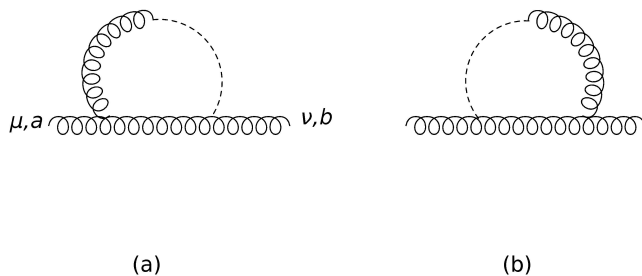


Figure 6: Loop formed by AAA , AB and ABB couplings;

Next we consider loops with the AAB vertex at one end and the ABB coupling at the other end. We find the diagrams shown in Fig. 7. The

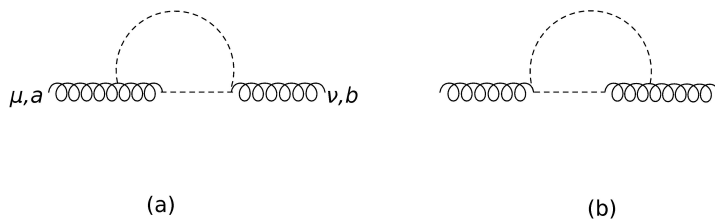


Figure 7: Loops formed by AAB , AB and ABB couplings;

divergent parts corresponding to these diagrams are equal, and are given by

$$\Pi_{ab,\mu\nu,\epsilon}^{7a} = -\frac{1}{2} \frac{N\delta^{ab}g^2}{16\pi^2} \frac{3}{2} m^2 g_{\mu\nu} = \Pi_{ab,\mu\nu,\epsilon}^{7b} \quad (25)$$

The factor $\frac{1}{2}$ for the diagrams in Fig. 7(a) and Fig. 7(b) is the symmetry factor for identical B -propagators in the loop.

Using the couplings AAA , AB , and ABB we get the diagrams shown in Fig. 8 and both diagrams give the same contribution,

$$\Pi_{ab,\mu\nu,\epsilon}^{8a} = -\frac{1}{4} \frac{N\delta^{ab}g^2}{16\pi^2} 3m^2 g_{\mu\nu} = \Pi_{ab,\mu\nu,\epsilon}^{8b} \quad (26)$$

Now there are identical A -propagators as well as identical B -propagators in each loop, so we pick up a symmetry factor of $\frac{1}{2} \times \frac{1}{2} = \frac{1}{4}$.

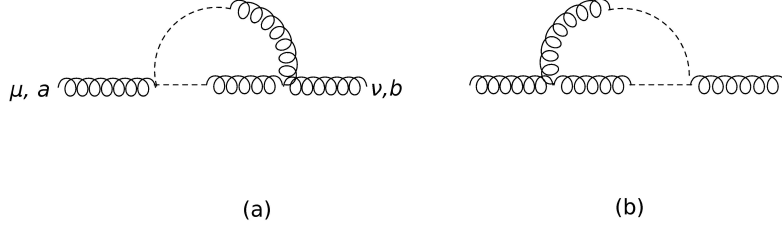


Figure 8: Loop formed by AAA , AB , and ABB couplings;

So the total contributions coming from the diagrams shown in Fig. 7 and Fig. 8 are

$$(\Pi_{ab,\mu\nu,\epsilon}^7 + \Pi_{ab,\mu\nu,\epsilon}^8) = -\frac{N\delta^{ab}g^2}{16\pi^2} 3m^2 g_{\mu\nu} \quad (27)$$

Only two more one loop diagrams remain. The $AABB$ interaction in the kinetic term of the $B_{\mu\nu}$ field leads to the diagram shown in Fig. 9(a), and the other diagram is Fig. 9(b), coming from the same interactions as in Fig. 7. The diagram in Fig. 9(b) is not divergent, so we can ignore it for our purposes.

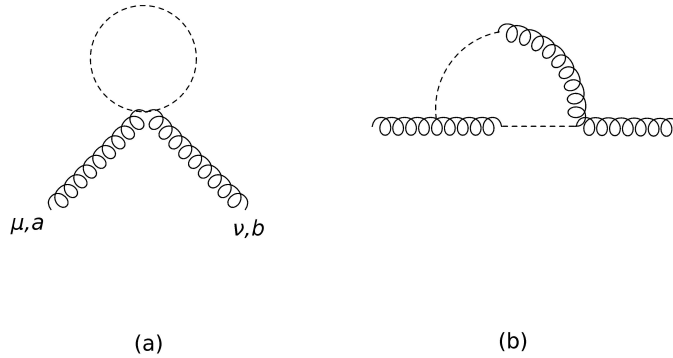


Figure 9: (a) Loop formed by $AABB$ couplings; (b) Loop formed by AAB , AB , and AAB couplings

The diagram in Fig. 9(a) contributes

$$\Pi_{ab,\mu\nu,\epsilon}^9 = -\frac{1}{2} \frac{N\delta^{ab}g^2}{16\pi^2} 18m^2 g_{\mu\nu} . \quad (28)$$

Adding up the divergent parts corresponding to all the diagrams from Fig. 5 – Fig. 9, we find

$$\Pi_{ab,\mu\nu,\epsilon} = \sum_{n=4}^9 \Pi_{ab,\mu\nu,\epsilon}^n = \frac{N\delta^{ab}g^2}{16\pi^2} \left[\frac{8}{3} (p^2 g_{\mu\nu} - p_\mu p_\nu) - \frac{45}{4} m^2 g_{\mu\nu} \right]. \quad (29)$$

4 Beta function

The exact propagator of the gauge field at the one-loop level is calculated by summing over insertions of the one-loop diagrams as in Fig. 10, corresponding



Figure 10: Exact gluon propagator at one loop

to the equation

$$\tilde{\Delta}_{\mu\nu} = iD_{\mu\nu} + iD_{\mu\alpha}i\Pi^{\alpha\beta}iD_{\beta\nu} + iD_{\mu\alpha}i\Pi^{\alpha\beta}iD_{\beta\gamma}i\Pi^{\gamma\delta}iD_{\delta\nu} + \dots, \quad (30)$$

where we have suppressed the gauge indices. The solid blob is what we have calculated so far in Sec. 3, the sum of one-loop diagrams which contribute to the A -propagator.

Looking at the one loop corrections we have calculated, we see that the general structure of the correction $\Pi^{\alpha\beta}$ is

$$\Pi^{\alpha\beta}(k) = \pi_1(k^2, m^2)(g^{\alpha\beta}k^2 - k^\alpha k^\beta) + \pi_2(k^2, m^2)m^2g^{\alpha\beta}. \quad (31)$$

This form is misleading, however. The pole in the propagator of Eq. (12) came from an infinite sum over massless propagators, with the two-point interaction inserted in between. If we want to find the correction in the pole, we ought to consider loop corrections to the two-point vertex of Fig. 1(a), as well as to the B -propagator, in addition to the A propagator. But it is not necessary to do that for our purpose. Our original goal was to calculate the β -function of the gauge coupling constant, let us see how that is related to the calculations we have done so far.

We started our calculations from the renormalized Lagrangian density in Eq. (4). The Lagrangian density for the counterterms is thus

$$\begin{aligned}
\mathcal{L}_{ct} = & (Z_3 - 1) \frac{1}{4} F_a^{\mu\nu} F_{\mu\nu}^a + (Z_1 - 1) \frac{1}{12} H_a^{\mu\nu\lambda} H_{\mu\nu\lambda}^a + (Z_m - 1) \frac{m}{4} \epsilon^{\mu\nu\rho\lambda} F_{\mu\nu}^a B_{\rho\lambda}^a \\
& + (Z'_2 - 1) \partial_\mu \bar{\omega}_a \partial^\mu \omega^a - (Z'_1 - 1) g f_{bca} A_\mu^b \partial^\mu \bar{\omega}^a \omega_c - (Z_3 - 1) \frac{1}{2\xi} (\partial_\mu A_a^\mu)^2 \\
& - (Z_1 - 1) \frac{1}{2\eta} (D_\mu B^{\mu\nu})^2. \tag{32}
\end{aligned}$$

The counterterms crucial to our calculations are the ones related to gauge invariance under SU(N) gauge symmetry. It is easy to check that the counterterm Lagrangian of Eq. (32) is invariant under a renormalized BRST symmetry, which implies that the SU(N) gauge symmetry remains unbroken. In particular, in the chosen gauge, the Slavnov-Taylor identity coming from the BRST transformation is the same as for usual (massless) Yang-Mills theory, showing that only the transverse part of the propagator gets a correction¹. This supports our earlier comment that loop corrections to the two-point coupling as well as to the B -propagator have to be taken into account in order to calculate π_2 .

On the other hand, the β -function for the gauge coupling constant is affected by the B -field only through the calculation of the renormalization constant Z_3 , which is related to π_1 . From Eqs. (29) and (32), we get

$$Z_3 = 1 + \frac{Ng^2}{16\pi^2} \frac{8}{3} \left[\frac{2}{\epsilon} - \ln \frac{m^2}{\mu^2} \right], \tag{33}$$

where μ is the subtraction point, and we have ignored a constant, independent of μ and m , in the second term.

In order to calculate the β -function for the gauge coupling constant, we need the relation between the gauge coupling constant at momentum scale μ with the bare coupling constant. If we add \mathcal{L}_{ct} with the renormalized Lagrangian given in Eq. (4), we find the bare Lagrangian density,

$$\begin{aligned}
\mathcal{L}_{\mathcal{B}} &= \mathcal{L} + \mathcal{L}_{ct} \\
&= -\frac{1}{4} F_{\mathcal{B}}^{\mu\nu a} F_{\mathcal{B}\mu\nu a} + \frac{1}{12} H_{\mathcal{B}}^{\mu\nu\lambda a} H_{\mathcal{B}\mu\nu\lambda a} + \frac{m_{\mathcal{B}}}{4} \epsilon^{\mu\nu\rho\lambda} F_{\mathcal{B}\mu\nu a} B_{\mathcal{B}\rho\lambda}^a \\
&\quad + \partial_\mu \bar{\omega}_{\mathcal{B}a} \partial^\mu \omega_{\mathcal{B}}^a - g_{\mathcal{B}} f_{bca} A_{\mathcal{B}\mu}^b \partial^\mu \bar{\omega}_{\mathcal{B}}^a \omega_{\mathcal{B}c}, \tag{34}
\end{aligned}$$

¹We thank the anonymous referee for asking for a clarification on this point.

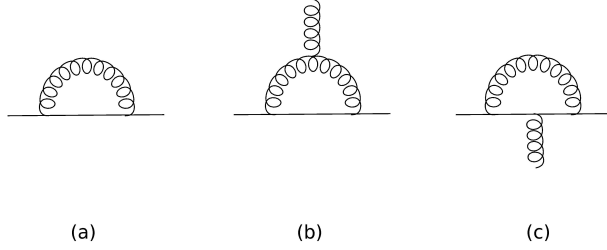


Figure 11: One loop contributions to Z'_1 and Z'_2

where

$$A_{\mathcal{B}} = Z_3^{\frac{1}{2}} A \quad (35)$$

$$B_{\mathcal{B}} = Z_1^{\frac{1}{2}} B \quad (36)$$

$$\omega_{\mathcal{B}} = Z_2^{\frac{1}{2}} \omega \quad (37)$$

$$m_{\mathcal{B}} = \frac{Z_m}{Z_3^{\frac{1}{2}} Z_1^{\frac{1}{2}}} m \quad (38)$$

$$g_{\mathcal{B}} = \frac{Z'_1}{Z_3^{\frac{1}{2}} Z'_2} g, \quad (39)$$

and the subscript \mathcal{B} denotes bare fields and coupling constants.

We consider the diagram Fig. 11(a) for the the one loop correction for the ghost propagator. It can be checked explicitly that the divergent part of this diagram, and thus Z'_2 , is unaffected by a massive pole in the gauge field propagator. Similarly it can be checked by explicit calculation that the mass does not affect the one loop corrections to the gauge-ghost vertex, and thus Z'_1 . The relevant diagrams are shown in Fig. 11(b) and 11(c).

The reasons are easy to understand by looking at the diagrams. The $A^\mu \bar{\omega} \omega$ interaction has the tree-level vertex rule

$$iV_{abc}^\mu = -gf_{bca} p^\mu, \quad (40)$$

where p^μ is the incoming momentum carried by the ghost field. The external momentum does not enter the loop integration, so the one loop divergence remains logarithmic as in usual Yang Mills gauge theory, and the pole does not contribute to the divergent part of Z'_2 . Similarly, the vertex correction contains three internal lines with three momentum dependent vertices, but

the divergent part of the loop integral comes from the leading power of the internal momentum. As a consequence, the loop divergence is also logarithmic. So the divergent parts of the renormalization factors are the same as in pure Yang Mills theory,

$$Z'_1 = 1 - \frac{Ng^2}{32\pi^2} \left(\frac{2}{\epsilon} - \ln \frac{m^2}{\mu^2} \right) \quad (41)$$

$$Z'_2 = 1 + \frac{Ng^2}{32\pi^2} \left(\frac{2}{\epsilon} - \ln \frac{m^2}{\mu^2} \right). \quad (42)$$

We can now calculate the beta function of $\alpha = \frac{g^2}{4\pi}$ using Eq.s (39), (33), (41) and (42),

$$\beta(\alpha) = \frac{\partial g(\mu)}{\partial \log \mu} = -\frac{14}{3} N \frac{\alpha^2}{2\pi}. \quad (43)$$

So the theory remains asymptotically free in spite of the appearance of a massive pole in the gauge field propagator due to the topological coupling.

5 Comments and conclusion

The main result of this paper is that non-Abelian gauge theory coupled to an antisymmetric tensor field is both short range and asymptotically free. We can think of the antisymmetric tensor as a minimally coupled matter field for the calculations done in this paper. In general, interaction with scalar and fermion fields has a screening effect for color charge, and the gauge coupling constant becomes flatter with respect to pure non-Abelian gauge theory, as the fields contribute positively to the beta function. But the interactions of the gauge field with the tensor field causes the coupling constant to fall away more steeply, as the additional contribution to the beta function is negative. We show in Fig. 12 the running of α as a function of Q using the relation

$$\alpha(Q^2) = \frac{\alpha(\mu^2)}{1 + N \frac{c}{\pi} \alpha(\mu^2) \ln \frac{Q^2}{\mu^2}}, \quad (44)$$

where $N = 3$, and $c = \frac{11}{12}$ for the pure massless Yang-Mills gauge field and $c = \frac{14}{12}$ for the topologically massive field considered in this paper. For the plot, we have taken $\mu^2 = M_Z^2$, with $\alpha(M_Z^2) = 0.12$ [14].

We did not consider quantum corrections to the propagator of the tensor field or to the two-point vector-tensor coupling. Consequently, we cannot make any comment on the renormalization of m in this theory. Dynamically generated gluon mass vanishes at short distances [6]. For the model we have considered here, the propagator has a pole and is well-behaved at short distances, in fact the gauge boson propagator in Eq. (12) behaves exactly like one with a dynamically generated mass [15]. We are unable to say at this point how m behaves at short distances in this model, but the form of the propagator, as well as the asymptotic behavior of α_s , indicates that the theory may be renormalizable, as has been argued algebraically elsewhere [13].

References

- [1] G. Aad *et al.* [ATLAS Collaboration], Phys. Lett. B **716**, 1 (2012) [arXiv:1207.7214 [hep-ex]].
- [2] S. Chatrchyan *et al.* [CMS Collaboration], Phys. Lett. B **716**, 30 (2012) [arXiv:1207.7235 [hep-ex]].
- [3] S. Weinberg, Phys. Rev. Lett. **19**, 1264 (1967).
- [4] A. Salam, Conf. Proc. C **680519**, 367 (1968).
- [5] A. C. Aguilar, D. Binosi and J. Papavassiliou, Phys. Rev. D **88**, 074010 (2013) [arXiv:1304.5936 [hep-ph]].
- [6] J. M. Cornwall, Phys. Rev. D **26**, 1453 (1982).
- [7] J. M. Cornwall, Nucl. Phys. B **157**, 392 (1979).
- [8] J. M. Cornwall, Phys. Rev. D **57**, 7589 (1998)
- [9] T. J. Allen, M. J. Bowick and A. Lahiri, Mod. Phys. Lett. A **6**, 559 (1991).
- [10] D. S. Hwang and C. -Y. Lee, J. Math. Phys. **38**, 30 (1997) [hep-th/9512216].
- [11] A. Lahiri, Phys. Rev. D **55**, 5045 (1997)
- [12] A. Lahiri and D. Mukhopadhyay, arXiv:1107.1501 [hep-ph].

- [13] A. Lahiri, Phys. Rev. D **63**, 105002 (2001) [hep-th/9911107].
- [14] J. Beringer *et al.* [Particle Data Group Collaboration], *Review of Particle Physics (RPP)*, Phys. Rev. D **86**, 010001 (2012).
- [15] A. C. Aguilar and J. Papavassiliou, Phys. Rev. D **81**, 034003 (2010) [arXiv:0910.4142 [hep-ph]].

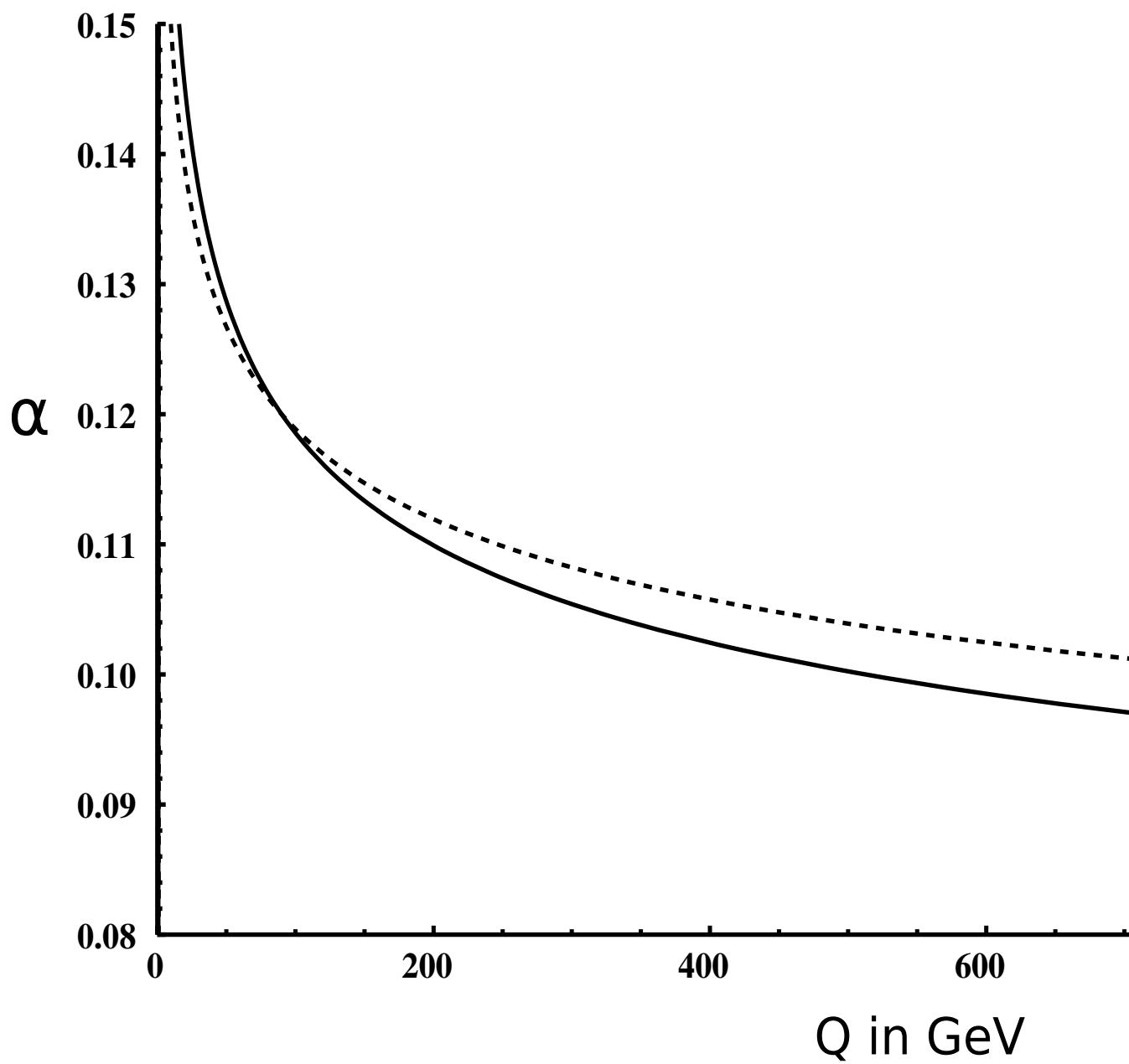


Figure 12: The flow of α_s for ordinary (dotted) and topologically massive (solid) SU(3) gauge theory.